



Assessing seasonal flow dynamics at a lagoon saltwater-freshwater interface using a dual tracer approach

Müller, Sascha; Jessen, Søren; Duque, C.; Sebök, Éva; Neilson, B.; Engesgaard, Peter

Published in:
Journal of Hydrology: Regional Studies

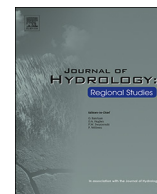
DOI:
[10.1016/j.ejrh.2018.03.005](https://doi.org/10.1016/j.ejrh.2018.03.005)

Publication date:
2018

Document version
Publisher's PDF, also known as Version of record

Document license:
[CC BY-NC-ND](#)

Citation for published version (APA):
Müller, S., Jessen, S., Duque, C., Sebök, É., Neilson, B., & Engesgaard, P. (2018). Assessing seasonal flow dynamics at a lagoon saltwater-freshwater interface using a dual tracer approach. *Journal of Hydrology: Regional Studies*, 17, 24-35. <https://doi.org/10.1016/j.ejrh.2018.03.005>



Assessing seasonal flow dynamics at a lagoon saltwater–freshwater interface using a dual tracer approach

S. Müller^{a,*}, S. Jessen^a, C. Duque^b, É. Sebök^a, B. Neilson^c, P. Engesgaard^a

^a Department of Geosciences and Natural Resource Management, University of Copenhagen, Denmark

^b Department of Geoscience, Aarhus University, Denmark

^c Department of Civil and Environmental Engineering, Utah State University, Logan, United States

ARTICLE INFO

Keywords:

Dual tracer

$\delta^{18}\text{O}$

$\delta^2\text{H}$

Salinity

Saltwater wedge dynamics

Saltwater freshwater interaction

ABSTRACT

Study region: Eastern shore of Ringkøbing Fjord, a coastal lagoon at the west coast of Denmark
Study focus: A dual tracer approach based on salinity and $\delta^{18}\text{O}$ is used to assess seasonal dynamics at the saltwater–freshwater interface of a coastal lagoon. At the site, salinity is prone to vary on a sub-seasonal or daily frequency due to riverine freshwater inputs to the lagoon. In contrast, $\delta^{18}\text{O}$ compositions of end-members only vary seasonally.

New hydrological insights: The dual tracer approach shows to be valuable in coastal settings where end-member concentrations vary substantially over the seasons and hence, an unambiguous end-member definition does not exist. Calculated mixing fractions using only salinity, deviated from the dual tracer approach on average by 18%, but were as high as 97%. Although, these differences decrease to 6% on average when using only $\delta^{18}\text{O}$, our study strongly suggests their simultaneous application.

Moreover, we found that seawater intrusion occurs during the summer when salinity in the lagoon is high and fresh submarine groundwater discharge (SGD) is low. This process reverses during the winter (wet season) when SGD increases by a factor of 2–3, due to the recession of the saltwater wedge from land. Our findings show that in absence of waves and tides, density-driven dynamics, and particularly the terrestrial freshwater fluxes, create a major impact on saltwater wedge dynamics.

1. Introduction

Coastal lagoons are an extreme form of barrier estuaries (Kjerfve, 1994; Haines, 2006) where hydrodynamic conditions are typically defined by the balance of tides and waves (Woodroffe, 2002), riverine freshwater inputs, precipitation, evaporation, and groundwater inputs (Phleger et al., 1981). All these factors are responsible for salinity dynamics (Kjerfve, 1994) and nutrient levels (Cartwright et al., 2004) in lagoon ecosystems. The interaction between groundwater and lagoons is similar to coastal systems. Coastal groundwater aquifers have been recognized as controls to nutrient supplies to estuarine systems (Burnett et al., 2001; Michael et al., 2003; Spruill and Bratton, 2008). The freshwater moving through the coastal aquifers discharges to the sea as terrestrial or fresh submarine groundwater discharge (SGD), and partly controls saltwater intrusion (Michael et al., 2005; Barlow and Reichard, 2010; Chang and Clement, 2012).

At the interface of fresh- and saltwater, density differences occur and a dynamic freshwater–saltwater mixing zone develops. In non-karstic field settings the width of such a mixing zone can vary from a few meters to kilometers (Barlow, 2003; Price et al., 2003;

* Corresponding author at: Øster Voldgade 10, 1350 Copenhagen, Denmark.

E-mail address: samu@ign.ku.dk (S. Müller).

Werner et al., 2013) and depends on the aquifer properties (geology, hydraulic properties), salinity of surface water, geological history of sea level, and groundwater abstractions (Barlow, 2003; Barlow and Reichard, 2010; Werner et al., 2013; Chang and Clement, 2012). The number of field studies investigating the temporal changes in the size of the mixing zone in shallow porous medium aquifers is limited (Werner et al., 2013). Most research has addressed the temporal dynamics of this interface due to tidal wave action via well salinity profiling and surface water observations (i.e., Kurup et al., 1998; Haralambidou et al., 2010) or numerical modelling (i.e., Ataie-Ashtiani et al., 1999). Cartwright et al. (2004) showed that the saltwater-freshwater interface could recede by several meters over a period of three days and then progress again by several meters over 10 days in response to storm wave activity. Only a few studies (Robinson et al., 1998; Michael et al., 2005) show that temporal dynamics of the mixing zone are an interplay between seasonal changes in surface water salinity, tidal amplitudes, and the hydrological cycle on land.

Periods with high recharge lead to increased freshwater inputs (measured as fresh terrestrial SGD) and increased hydraulic heads in the near-coastal aquifer, causing the freshwater-saltwater interface to move towards the sea. During periods of lower fresh terrestrial SGD, but higher sea or lagoon water salinity, the opposite occurs and the saltwater interface intrudes further inland (Poulsen et al., 2010). Likewise, the timing of maximum salinity in the surface water and maximum freshwater discharge affects the interface dynamics. In low-lying areas of temperate climate, maximum freshwater SGD typically occurs between late fall and the middle of winter when surface water salinity in lagoons can be low due to high riverine freshwater inputs. During the summer, the opposite situation occurs with maximum surface water salinity and minimum freshwater SGD. Further complexity to the interface dynamics is added by the heterogeneous nature of aquifers and sediment water interfaces, yielding increased spatial variability of SGD (Taniguchi et al., 2002; Burnett and Dulaiova, 2003; Duque et al., 2016). Nonetheless, there are few field studies in coastal systems where wave and tidal activity are limited. In such systems, flow dynamics are highly controlled by the seasonal changes in groundwater inputs and density differences between the surface and groundwater.

This leaves the responses of lagoons to future hydrologic changes poorly understood even though approximately 60% of Europe's coastline fits within this classification with mean tidal amplitudes below 0.5 m (Data from EEA, 2012). Hence, a substantial part of saltwater intrusion dynamics on Europe's coastline is likely controlled by the density dynamics within aquifers and the temporal offset dynamics of the continental freshwater flux, and salinity of lagoons, rather than wave or tidal activity. By understanding saltwater intrusion within these coastlines, we can further understand the temporal character of total terrestrial discharge estimates and, thus, its corresponding nutrient loads. Furthermore, understanding these density dynamics in aquifers at a small scale helps to improve or refine simulation models that further enables transferability of models to larger scales.

The complex nature of the saltwater-freshwater interface requires a set of methods to be applied, that can appropriately characterize such dynamics. Physically-based methods such as seepage meters and hydraulic head observations have been used for many years in coastal situations (Lee, 1977). In order to evaluate the intrusive characteristics of saltwater in coastal areas, these methods have to be extended with reactive and conservative chemical and isotopic tracers (Burnett et al., 2006). Although salinity is the obvious choice in coastal settings it may not be appropriate when there are large salinity changes in end members over time. This can cause high uncertainty in mixing predictions and therefore mislead the conceptual understanding of coastal subsurface flow dynamics. In many cases, salinity may vary substantially over different temporal scales (annually, monthly, daily) due to dilution with freshwater, and/or chemical conditions at the location (e.g. calcite dissolution of carbonate rocks). In such environments, the water stable isotopes of ^{18}O and ^2H may be a robust tracer. $\delta^{18}\text{O}$ in surface and terrestrial waters is mainly influenced by temperature and evaporation processes that occur on an annual basis (Clark and Fritz, 1997; Kendall and Caldwell, 1998) and the variations in temperate climate zones are minor, compared to arid regions. $\delta^{18}\text{O}$ and $\delta^2\text{H}$ variations in groundwater effectively damp out seasonal variations of meteoric waters due to long travel times and enhanced mixing in aquifers (Leibundgut et al., 2009). Hence, water stable isotopes of ^{18}O and ^2H provide an effective labelling of seawater and freshwater and enables an understanding of seawater intrusion and mixing ratios. Moreover, the relationship between ^{18}O and ^2H with salinity is well established (Yurtsever, 1997; Clark and Fritz, 1997) as $\delta^{18}\text{O}$ and salinity are generally known to (a) increase with evaporation, (b) decrease with higher precipitation or other freshwater inputs and (c) vary by mixing from advection and diffusion processes. As the controlling processes depend on season, climate and geographic location, the slope and intercept of ^{18}O -salinity relation may vary seasonally and geographically (Benway and Mix, 2004; McConnell et al., 2009; Singh et al., 2010). Most importantly their stability at different temporal scales make them complementary to conservative tracers, which decreases the uncertainty in mixing estimations. Due to advances in the measurement techniques for stable water isotopes and the ease to obtain salinity estimates, these two tracers are also cost efficient.

Along these lines, this study (i) explores the use and benefits of salinity and water stable isotopes (dual tracer approach) over the use of only one of these tracers, and (ii) supplement this dual tracer approach with direct physical measurements (head gradients, seepage rates) to further understand the seasonal dynamics of the lagoon saltwater-freshwater interface in the absence of tides and wave activity.

The Ringkøbing Fjord system in Denmark is investigated, where the lagoon water is characterized as brackish water and is subject to seasonal salinity changes due to seasonal changes in discharge from the largest river in Denmark (Skjern River). As tides and wave activity are negligible, the field site provides great field laboratory conditions to study density driven dynamic processes.

2. Study site

The study site is located at the eastern shore of Ringkøbing Fjord at the west coast of Denmark (Fig. 1A). The fjord can be characterized as a restricted lagoon system (Kjerfve, 1994). It has an area of 300 km² and although it has a mean water depth of 1.9 m, more than 25% of the area is less than 0.5 m deep (Kirkegaard et al., 2011; Kinnear et al., 2013). At its western extent, the lagoon is disconnected from the ocean through a natural barrier (Haider, 2013). A man-made channel that is regulated by a lock is the

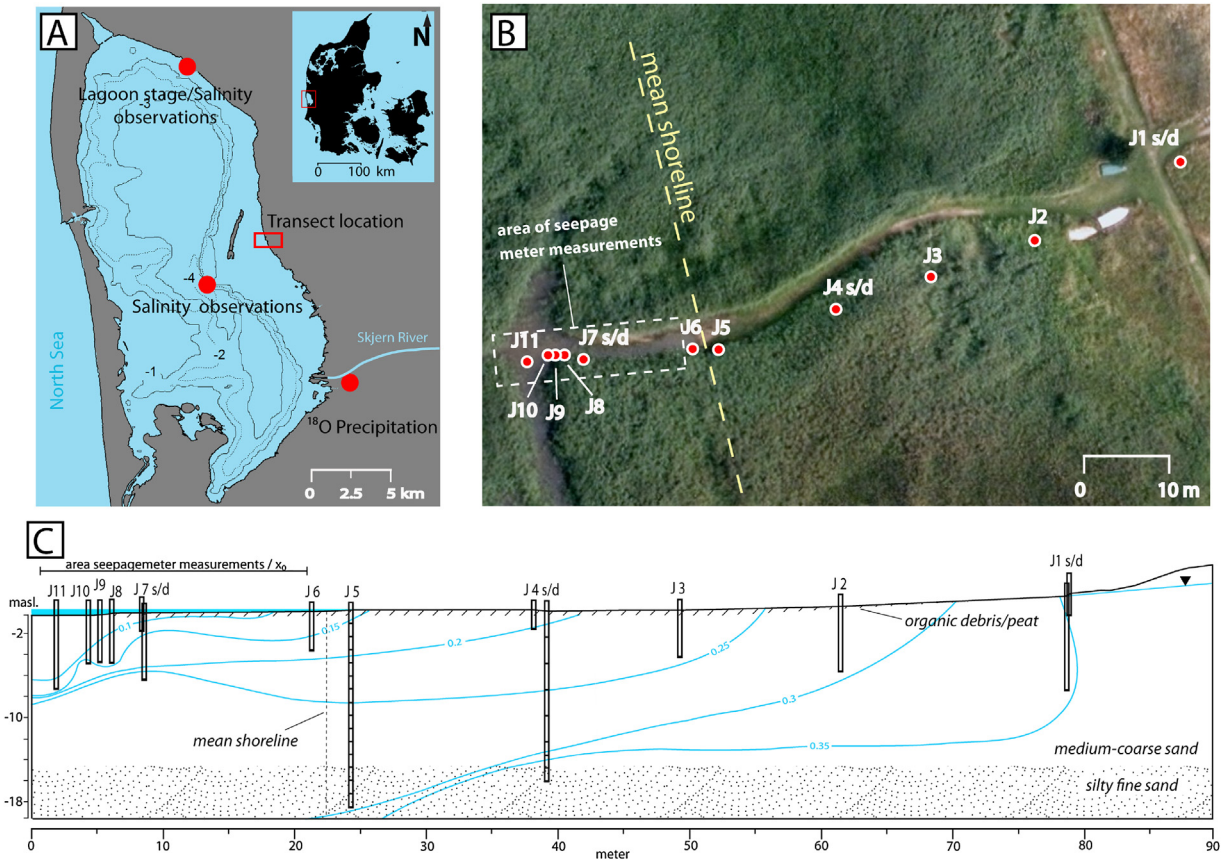


Fig. 1. (A) Location of field site. Measurement location of lagoon stage/salinity and $\delta^{18}\text{O}$ in precipitation sampler. (B) Aerial view of field site showing wells, seepage meter and mean shore line locations. Subscripts 's' and 'd' describe the relative depth being shallow or deep, respectively. (C) Cross-section of transect including an average iso-potential map based on head measurements (averaged from October '14–July '15). Vertical lines within and at the end of piezometer sketch indicate sampling points and final screen locations.

only surface connection between the ocean and the lagoon. This channel maintains the water level in the lagoon at approximately 0.25 m above sea level (m.a.s.l.) and salinity values between 6 and 15‰. The lagoon receives freshwater inflow from Skjern River with an annual mean discharge of $50 \text{ m}^3/\text{s}$ (Kirkegaard et al., 2011; Haider, 2013) at its south-eastern extent. Discharge data from a discharge station (Stat. Nr. 250097) located 16 km upstream of the effluent indicates a seasonal discharge distribution of low flows during summer months (May–Aug.) and high flows during the winter months (Dec.–Jan.). Minor freshwater inputs from drainage systems at the eastern shoreline are also present. Airborne and waterborne geophysical surveys have provided information on groundwater interacting with the lagoon and have shown that groundwater inflow occurs mainly along the eastern shoreline with a highly variable pattern and magnitude, but it is also expected at the northern and southern shore (Kirkegaard et al., 2011). Groundwater discharge zones are generally located within tens of meters from the shoreline and most often occurring in micro-bays along the shore (Kirkegaard et al., 2011; Kinnear et al., 2013). Nevertheless, there is evidence for further offshore terrestrial SGD zones (Kirkegaard et al., 2011; Haider et al., 2014). Groundwater input to the lagoon system was estimated to be $14.5 \text{ m}^3/\text{d}$ per meter shoreline by numerical modelling for the 40 km eastern shoreline, which corresponds to 17% of the total discharge from Skjern River (Haider et al., 2014). This estimate is highly uncertain as its spatial extent and volume strongly depends on aquifer heterogeneities. Local measurements using temperature as a tracer has estimated a mean flux of $0.026 \text{ m}/\text{d}$, but can vary between 0.07 to below $0.01 \text{ m}/\text{d}$ (Duque et al., 2016). If one assumes a discharge width of 20 m, the mean flux translates into a terrestrial input of $0.52 \text{ m}^3/\text{d}$ per meter shoreline, much less than predicted by the model of Haider et al. (2014).

The study site on the eastern shore consists of a shallow, sandy phreatic aquifer containing Pleistocene fluvial-glacial sands. It includes an area roughly 25 m off-shore and 65 m in-land (Fig. 1B). The onshore elevation (up to well J1) is less than 1 m.a.s.l. followed by a short steep slope increasing the elevation to 3 m.a.s.l. (Fig. 1C). The regional aquifer is intervened by low permeability silty units and high permeability paleo-channels (Haider, 2013). A confining lower permeable unit is present at about 12 m depth. The vegetation has adapted to the brackish water conditions and grows across the shoreline with greater density onshore and in patchy areas offshore.

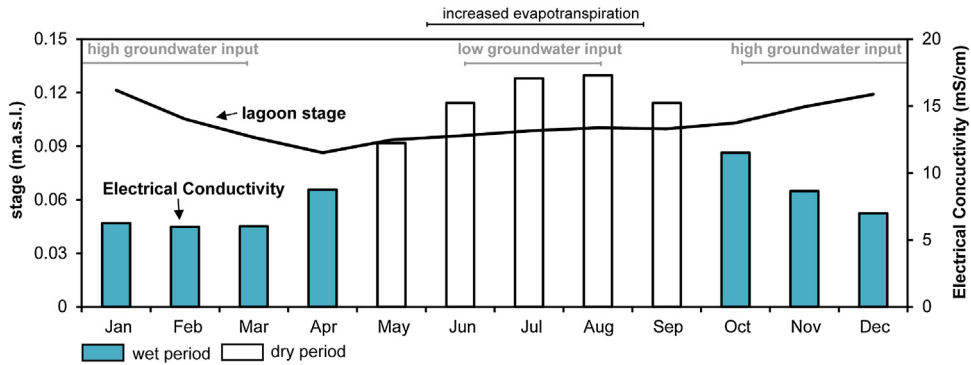


Fig. 2. Seasonal variations of lagoon stage and salinity (expressed as EC). Data are monthly averages between 1998 and 2015.

3. Data and methods

3.1. Hydrogeology

A 90 m long transect of 14 piezometer wells was established perpendicular to the shoreline (Fig. 1B). Based on earlier studies (Haider et al., 2014; Duque et al., 2016) the saltwater intrusion was expected to be located within this area. The wells were screened (0.1 m screen length) at different depths ranging from 1.3 m to 15 m below the surface. They were assembled from 2 m long stainless steel pipes of 1 in. diameter and connected by steel fittings sealed with Teflon tape. Hydraulic heads, water stable isotopes and Electrical Conductivity (EC) were measured in October 2014, February, April and July 2015 in all wells. Reported hydraulic heads are corrected for density effects according to Post et al., 2007. Additionally, at wells J4d and J5 (Fig. 1B), vertical tracer profiles were established in October 2014 and February 2015, respectively, taking samples with one meter resolution. Three casing volumes were purged from each well prior to sampling. Single measurements from the Lagoon water isotopic compositions were available from previous years for August 2010 and May 2012. Samples obtained in October, February and April are grouped as wet season samples and July and August samples are grouped as dry season samples according to the temporal variation of annual precipitation amounts.

3.2. Lagoon stage and salinity

Data on the lagoon stage was available from September 1998–2015 from a station in the lagoon north of the field site (Fig. 1A) and was provided by the Danish coastal authority. The lagoon stage varied between 0.07 m.a.s.l. during early spring to 0.13 m.a.s.l. in December. Salinity and EC measurements were provided by the Danish Nature Agency also from 1998–2015 (Fig. 1A). A data gap existed only for EC data between 2000 and 2009. Consequently, these dates were excluded from the analysis. The highest average EC of 17 mS/cm is typically observed during summer months, while EC in winter months is around 6 mS/cm (Fig. 2).

3.3. Seepage meter measurements

Seepage meter measurements were conducted near the offshore wells (Fig. 1B). Measurements took place in October 2014 (wet period) and July 2015 (dry period). The seepage meters were constructed after Lee (1977) with a half barrel of 0.25 m² inflow area. A collection bag was attached to a valve connected to the top of the barrel to control the inflow manually. The bag was protected from the limited wave activity by a plastic box. The bag was pre-filled with at least 15% of the total bag volume. Each location was measured three times.

3.4. Groundwater electrical conductivity (EC) and stable isotopes

The EC of the lagoon is to a great extent controlled by the incoming seawater through the lock and discharge from Skjern River with small daily and high yearly amplitudes in the range of brackish water (Fig. 2). The EC in groundwater is expected to be relatively stable at low values producing a large contrast to the lagoon water. Increased saltwater intrusion into the groundwater may be expected during summer due to higher salinities in the lagoon. In contrast, retreating saltwater is expected during the winter, when salinity is lower in the lagoon. Both processes are affected by terrestrial freshwater fluxes as hydraulic gradients are smallest during summer and highest during winter. The $\delta^{18}\text{O}$ composition of the incoming fresh groundwater would be expected to remain stable. Evaporation in summer causes an isotopic enrichment of the lagoon water by several permil compared to groundwater. That enrichment remains stable throughout the summer season due to the long water residence times of water in the lagoon. Hence, $\delta^{18}\text{O}$ is potentially a better tracer than EC with more robust and stable end-member compositions. Water samples from the lagoon, wells, and seepage meters were analyzed for EC and $\delta^{18}\text{O}/\delta^{16}\text{O}$ isotopes. EC measurements were taken with a calibrated WTW Cond 3310. The salinity concentration (S in g/L) is calculated from EC at 25 °C using the empirical equation from Holzbecher (1998):

$$S \text{ (mg/L)} = -3.83 + 0.699 \cdot \text{EC} \text{ (}\mu\text{S/cm)} \quad (1)$$

Samples for isotope analysis were filtered through a 0.45 μm Nylon filter and analyzed for $\delta^{18}\text{O}$ ($\pm 0.1\text{‰}$) and $\delta^2\text{H}$ ($\pm 0.2\text{‰}$) by the cavity ring down spectroscopy method using a PICARRO L2021-i at the Geological Survey of Denmark and Greenland (GEUS), Copenhagen. The δ -notation given in ‰ is the relative deviation from the Vienna-Standard Mean Ocean Water (V-SMOW) standard (Craig, 1961).

3.5. Mixing analysis

A mixing analysis was carried out using the software package MIX (Carrera et al., 2004). It uses a maximum-likelihood method to calculate mixing ratios accounting for the uncertainty of the end-members (EM's) and samples. This EM uncertainty arises from concentration variations in space and time and from analytical errors. Two EM's were identified (lagoon water, groundwater) which differ in their isotopic composition and EC. One EM represents the recharge/groundwater composition entering the transect from east. Hence, the groundwater EM composition is assumed to be represented by the average $\delta^{18}\text{O}$ composition of meteoric water (Clark and Fritz, 1997) and a salinity (expressed in EC (mS/cm)) deduced from the shallow onshore wells J1–J4.

The lagoon EM concentration for EC was represented by the average observed measured EC between 1998–2015. Assuming that enhanced saltwater intrusion mainly occurs at the time of highest salinity (summer), the isotopic EM was chosen based on $\delta^{18}\text{O}$ samples from previous summers and late spring (August 2010, May 2012) and combined with current observations of lagoon water from July 2015. The assigned variances for both EM compositions are deducted from the standard deviation of the annual changes of groundwater and lagoon water (see later).

For comparison, a classical simple linear end-member mixing analysis (EMMA) was also applied, where only a single parameter (i.e., either EC or $\delta^{18}\text{O}$) was used and an observed fraction of lagoon water in a sample (f_{lag}) was established based on conservative linear mixing process between two EM's (Apello and Postma, 2005):

$$f_{\text{lag}} = \frac{m_{\text{sample}} - m_{\text{freshwater}}}{m_{\text{lag}} - m_{\text{freshwater}}} \quad (2)$$

where m_{sample} is the parameter value in the sample, and $m_{\text{freshwater}}$ and m_{lag} are the EM values of the groundwater and lagoon water, respectively.

4. Results and discussion

4.1. Hydraulic head gradients and seepage meter fluxes

Maximum and minimum lagoon stages in the observational period ranged between 0.07 and 0.13 m.a.s.l. (Fig. 3). All onshore wells (J1–J5) show a hydraulic gradient from land towards the lagoon. The average hydraulic head observations (Fig. 1C) show that groundwater flows into the transect site and is confined by the lower-permeable silty (bottom) and organic layers (surface) causing artesian conditions. Nevertheless, seasonal head fluctuations exist (Fig. 3). Those fluctuations are higher for offshore wells (J6–J11) than onshore wells (J1–J5) and a result of density dynamics in the subsurface of the lagoon. This causes offshore hydraulic heads occasionally to be above onshore hydraulic heads. Thus, a dynamic interface is developed, where positive hydraulic gradients (groundwater flow into the lagoon) may partly be reversed and lagoon water is able to flow into the onshore groundwater body.

Seepage meter fluxes from autumn and summer always show discharge from the aquifer into the lagoon (Fig. 3). The average discharge in October is 3.7 cm/d with a high seepage occurring close to the shore (5 cm/d) followed by a decrease 5–15 m offshore and a high seepage 15–23 m offshore. The fluxes during July 2015 are lower than in October with an average discharge of 1.6 cm/d. The lowest seepage is observed near the shore with increased seepage fluxes further offshore. Higher seepage fluxes in October can be linked to higher hydraulic gradients, while the lower fluxes in July correspond to lower hydraulic gradients. Nonetheless, this relation may be modified as recirculating groundwater can amplify seepage rates (Li et al., 1999; Taniguchi et al., 2002).

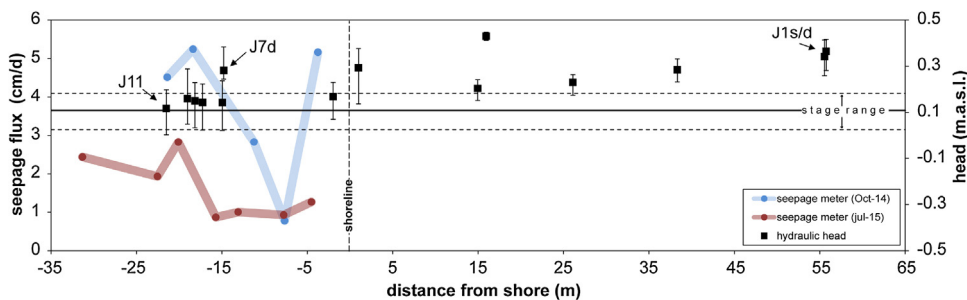


Fig. 3. Hydraulic heads and seepage meter fluxes (October 2014 and July 2015) given as average values. Average of hydraulic heads calculated from measurements from Oct.'14, Feb.'15, Apr.'15 and Jul.'15 and corrected for density effects after Post et al. (2007). Error bars for hydraulic heads correspond to observed minimum and maximum values (across all seasons). Maximum/minimum lagoon stage is indicated by the dotted line.

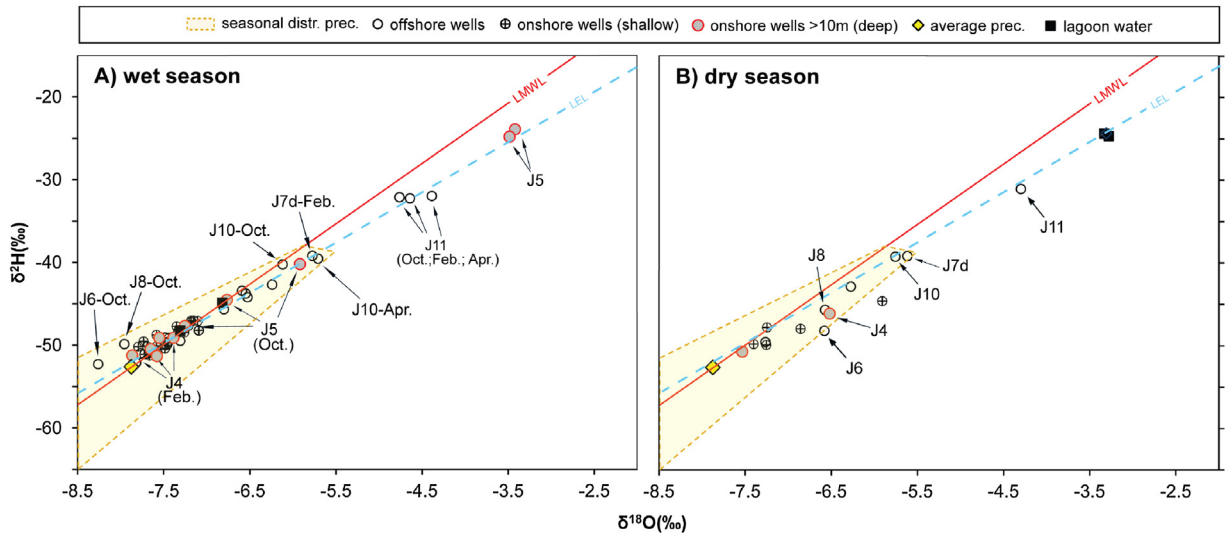


Fig. 4. Dual isotope plot ($\delta^{18}\text{O}$ – $\delta^2\text{H}$): (A) wet season samples (Oct.'14–Apr.'15), (B) dry season samples (Aug.'12, Jul.'15). Local Meteoric Water Line (LMWL) established by Müller et al. (2017). Local evaporation line (LEL) is developed based on all lagoon $\delta^{18}\text{O}/\delta^2\text{H}$ samples. The seasonal distribution of precipitation (yellow area) surrounds the area in which all precipitation samples from the nearby station plot (2012–2015).

4.2. Water stable isotopes and salinity

The $\delta^{18}\text{O}$ isotopic composition of precipitation in the area ranges between -5.5‰ (38.3‰ $\delta^2\text{H}$) and -10‰ (-73.4‰ $\delta^2\text{H}$) with an average of -7.8‰ $\delta^{18}\text{O}$ (-52‰ $\delta^2\text{H}$) (Fig. 4). A local meteoric water line (LMWL) for the area of -7.29‰ $\delta^{18}\text{O} + 4.81\text{‰}$ has been established on the basis of precipitation measurements at the nearby station (Müller et al., 2017) (Fig. 1A). Most enriched values are observed during early spring while most depleted values are observed during winter (Müller et al., 2017). The lagoon water samples from the wet period (October–April) plot along the LMWL, whereas the dry season samples (May–August) plot below the LMWL with more enriched values. This is consistent with an evaporation of lagoon water during summer and higher freshwater inputs to the lagoon with less evaporation during other seasons. Salinity effects on the fractionation process during evaporation, as postulated for brine water or hypersaline environments (Gonfiantini, 1986; Gat, 2010), are not expected due to the low salinity characteristics of the lagoon.

Combining lagoon samples from both seasons, a local evaporation line (LEL) is developed with a slope lower than the LMWL of 6.02 and an intercept value of -4.43‰ . This is a typical slope for evaporating seawater (Gat, 2010). For the August 2012 sample, no $\delta^2\text{H}$ was available, hence it was excluded for the development of the LEL. However, its corresponding deuterium value was calculated from the LEL regression (this assumes similar evaporation conditions in 2012) in order to be shown (Fig. 4).

All groundwater samples (onshore and offshore wells) are on average 1‰ more enriched in $\delta^{18}\text{O}$ (-6.91‰ $\delta^{18}\text{O}$, -46.2‰ $\delta^2\text{H}$) than the average rain composition. The range of the groundwater composition is between -8.26‰ $\delta^{18}\text{O}$ (-52.2‰ $\delta^2\text{H}$) at J6 in October to -3.42‰ $\delta^{18}\text{O}$ (-23.9‰ $\delta^2\text{H}$) at J5 in October, where the $\delta^{18}\text{O}$ at J5 indicates intruding saltwater. Yet, the majority of the samples plot more closely along the LEL than the LMWL. The bulk of the groundwater samples from the onshore wells in the wet season plot close to the average value of precipitation. This may be an indication of its meteoric origin, with enhanced regional freshwater contribution in wet periods.

As shown above, lagoon water undergoes evaporative enrichment during summer. The offshore well, J11, always plots along the LEL as it is distinctively enriched compared to other offshore wells. This indicates the presence of summer-intruded lagoon water. Independent of season, J7d and J10 also show enriched isotopic compositions, but are lower than J11. This is likely due to the screen location being within the saltwater-freshwater transition zone, where samples from J7d and J10 are subject to mixing dynamics of a large portion of intruding lagoon water from above and less influence of fresh groundwater coming from land. Samples from J6 and J8 in October are the most depleted samples in the wet period and also show the least enrichment during dry season. Hence, these samples suggest to sample water in the saltwater-freshwater transition zone, but with a strong freshwater influence mixed with a smaller amount of lagoon water. Additional information on the saltwater wedge extension can be delineated from the isotopic composition. Groundwater samples at depths greater than 10 m plot along the LEL. The onshore well J4d plots around the mean groundwater value. Contrary to this, samples from J5 in the wet period, close to shore, plot between the most enriched lagoon samples and the intersect of the LEL and LMWL. Hence, during the wet season, the saltwater wedge is expected to be located between wells J5 and J4 and should have a relatively steep slope. Because not all depths from J5 and J4 were sampled, no information on the exact toe location can be given.

The relation between the $\delta^{18}\text{O}$ and salinity serves as a basis to deduce end-members. Lagoon water ultimately is a mixture of freshwater inputs (GW) to the lagoon and seawater from the North Sea (SW). Fig. 5 therefore indicates a mixing line (GW–SW mix) between a freshwater end-member (zero salinity, -7.8‰ $\delta^{18}\text{O}$ from the average of precipitation) and oceanic seawater (35 g/L

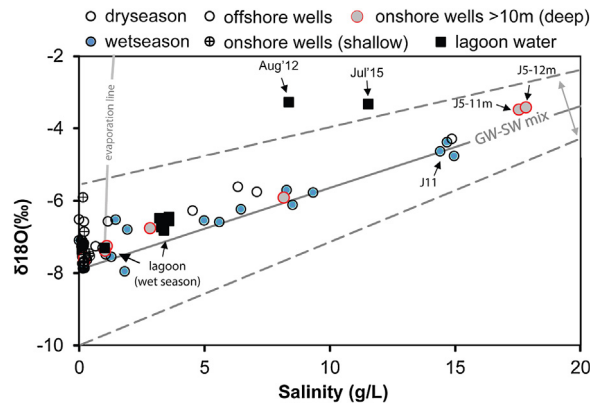


Fig. 5. $\delta^{18}\text{O}$ (‰)- salinity (g/L) plot. Mixing line range between average (groundwater–seawater mixing [GW–SW mix]), maximum and minimum $\delta^{18}\text{O}$ composition of freshwater (< 0.2 g/L). Evaporation line composed of evaporative enrichment calculated after (Gonfiantini, 1986) using humidity of 65% (measured min. summer observation at $\delta^{18}\text{O}$ precipitation station, Fig. 1). Minimum observed lagoon composition ($\delta^{18}\text{O}$ /salinity) was used as starting point of evaporation line. Salinity estimated from EC using the relation described in Section 3.4.

salinity (DMI, 2017), 0‰ $\delta^{18}\text{O}$). As a consequence of the seasonal variation of $\delta^{18}\text{O}$ in precipitation, a potential range in mixing is indicated by the dashed lines. When evaporation from an open water body occurs, a steep increase in the $\delta^{18}\text{O}$ of the remaining water will be accompanied by a relatively small increase in salinity (Gonfiantini, 1986). This $\delta^{18}\text{O}$ -salinity relation during evaporation is illustrated by the evaporation line in Fig. 5 (see details in Figure). The lagoon water plots distinctively different (Fig. 5) for different seasons. Wet season samples are close to that of groundwater. Dry season samples are outside the GW–SW mixing range and instead fall between the evaporation line and the mixing range. This points towards evaporative enrichment (Gonfiantini, 1986) of the lagoon water during summer months.

All shallow onshore wells have very low salinity (< 0.3 g/L) and $\delta^{18}\text{O}$ above the average value of precipitation (Fig. 5). The offshore wells, deep onshore wells, and wet season lagoon water plot along the GW–SW mixing line. However, the samples at 11 m and 12 m depth from J5 show a composition on the right end of the GW–SW mixing line, yet not close to lagoon water. Similar trends are seen for J11, independent of the season, suggesting that deep J5 and J11 samples are partially composed of North Sea water rather than lagoon water. Nonetheless, the dual isotope plot (Fig. 4) illustrates that these samples plot close to lagoon water, suggesting an opposite result. However, from the conceptual understanding of the system, it is more likely that deep J5 and J11 samples are biased towards the faster changing salinity in the lagoon. Hence, they are not capable of reflecting salinities similar to those observed in the lagoon. On the other hand $\delta^{18}\text{O}$ due its stability serves as a better predictor for the seawater composition at J5 and J11.

4.3. Mixing analysis

Two end-member mixing analysis was carried out for the wet season periods of October '14, February '15 and April '15 and for the dry period July '15. The assigned input values and variances are based on the average and standard-deviation of samples and end-members. The $\delta^{18}\text{O}$ composition of both EM lagoon and groundwater can be considered relatively stable with a variation by 1.09 and 0.01‰, respectively. The EC of groundwater can also be considered stable, while the variance of 4.5 mS/cm expresses the observed seasonal variation in the lagoon water (Table 1). This indicates the added advantage of using $\delta^{18}\text{O}$ as a more robust and stable tracer. The mixing model always forces the EC of the lagoon EM-composition to be higher than the average value in order to fit the observations. EC values are estimated to be between 18 mS/cm in February and 24 mS/cm in October, which is much higher than the average input value of 11.7 mS/cm. The $\delta^{18}\text{O}$ composition appears to be more stable, but is forced to be more depleted with ranges between 0.1‰ and 1‰. The smaller error introduced with $\delta^{18}\text{O}$ compared to EC promises more stability in the calculation and suggests the right EM choice of $\delta^{18}\text{O}$. As the average simulated lagoon-EM concentration of EC was always increased, it suggests that the initial use of an average value may be biased and the true EM concentration could be higher. Values in the range of modelled EC EM values are exclusively observed during the summer (as shown in Fig. 5), which fits the actual timing of the greatest saltwater intrusion. Nonetheless, a value of 24 mS/cm calculated for the lagoon EM in October has not been observed.

The results from the linear EMMA (either EC or $\delta^{18}\text{O}$) show a high deviation compared to the results of the dual end-member approach (Fig. 6). The EC tends to be over predicting, while $\delta^{18}\text{O}$ under predicts lagoon water fractions. The outcome of the linear EMMA is shown to be sensitive to the choice of EM composition. An average EM choice results in fractions far above 100%. This suggests incorrect EM values for the EMMA analysis. Furthermore, it highlights the advantage for two or more species for mixing analysis. Assuming that the MIX-model results in most certain fractions, the use of one tracer can be highly biased (i.e. choosing EC over $\delta^{18}\text{O}$, Fig. 6). When only EC is used and compared to MIX-fraction estimates, the two approaches yield an average difference of 18% for single wells with a standard deviation (stdv.) of 33%. In extreme cases, a well may contain 3% lagoon water based on the MIX model, but 100% lagoon water based on the EC end-member estimation. When using $\delta^{18}\text{O}$ instead these differences decrease on average to 6% with a stdv. of 7%. Hence, errors by choosing $\delta^{18}\text{O}$ for linear EMMA are smaller. In general, the results show the

Table 1

End-member (EM) estimation and fractions of lagoon water (%) estimated with the MIX-model. Model required EM input and EM variance are derived from average and standard deviations of the annual groundwater and lagoon water compositions. Measured values for $\delta^{18}\text{O}$ and EC were used for piezometer input. The analytical error was used for $\delta^{18}\text{O}$ variance, while the variance of EC was assumed 5% of the measured value. ‘**’ is used when data from the Nature Agency Denmark from 1998–2015 was used. October, February, April and July values is modelled output data.

| | Assigned input | | Assigned variance | | October | | February | | April | | July | |
|-----------------------------|---------------------------|--------------------|---------------------------|--------------------|---------------------------|--------------------|---------------------------|--------------------|---------------------------|--------------------|---------------------------|--------------------|
| | $\delta^{18}\text{O}$ [‰] | EC [mS/cm] (S [‰]) | $\delta^{18}\text{O}$ [‰] | EC [mS/cm] (S [‰]) | $\delta^{18}\text{O}$ [‰] | EC [mS/cm] (S [‰]) | $\delta^{18}\text{O}$ [‰] | EC [mS/cm] (S [‰]) | $\delta^{18}\text{O}$ [‰] | EC [mS/cm] (S [‰]) | $\delta^{18}\text{O}$ [‰] | EC [mS/cm] (S [‰]) |
| EM | –3.48 | 11.72 (4.36)* | 1.09 | 4.49 (3.14)* | –3.62 | 24.0 (12.94) | –4.45 | 18.14 (8.85) | –4.41 | 19.41 (9.74) | –4.36 | 19.35 (9.70) |
| Lagoon | –7.71 | 0.27 (–3.64)* | 0.01 | 0.13 (0.09)* | –7.65 | 0.12 (–3.75) | –7.54 | –0.29 (–4.03) | –7.69 | 0.17 (–3.71) | –7.40 | –0.45 (–4.15) |
| GW | | | | | | | | | | | | |
| % of lagoon water in sample | | | | | | | | | | | | |
| J1S | | | | – | | 2.1 | | | | | | 0 |
| J1D | | | | – | | 2.3 | | | | | | 0.2 |
| J2 | | | | 1.1 | | 2.1 | | | | | | 0.6 |
| J3 | | | | 0.1 | | 2.1 | | | | | | 0 |
| J4S | | | | 0.2 | | 2.2 | | | | | | 0.1 |
| J4D | | | | – | | 8.8 | | | | | | 8.6 |
| J5 | | | | – | | – | | | | | | 0.7 |
| J6 | | | | – | | 2.4 | | | | | | 0.3 |
| J7S | | | | – | | 2.8 | | | | | | 0.5 |
| J7D | | | | 55.1 | | 13.1 | | | | | | 40.1 |
| J8 | | | | 10.2 | | 3.4 | | | | | | 7 |
| J9 | | | | 38 | | 8.2 | | | | | | 36 |
| J10 | | | | 50 | | 16.4 | | | | | | 60.6 |
| J11 | | | | 87.6 | | 100 | | | | | | 100 |

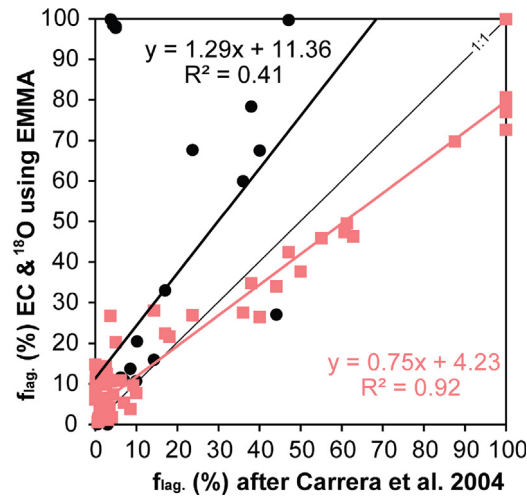


Fig. 6. Comparison of mixing fractions (f in %) of lagoon water from the MIX model approach (Carrera et al., 2004) with the linear EMMA using EC (black dots) or linear EMMA using $\delta^{18}\text{O}$ (red square). Fractions above 100% are not shown by the plot.

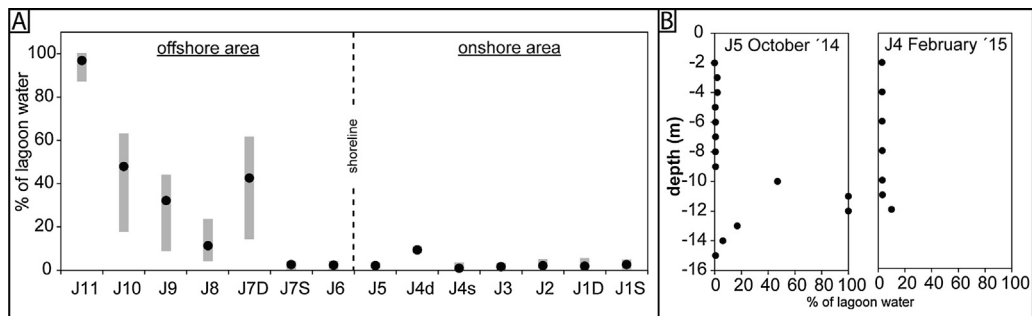


Fig. 7. (A) Average fraction of lagoon water across all seasons in single wells along transect. Fractions are established from the MIX-model approach using two species simultaneously ($\delta^{18}\text{O}$, EC). Results are averaged over all seasons and error bars indicate the minimum and maximum fractions (%). (B) Fractions of lagoon water in two profile wells. Only one measurement was taken for each depth at the specific point in time.

advantage of a MIX model analysis over the EMMA approach. On the basis of these results the EMMA analysis is not considered in the following.

From the average mixing fractions (Fig. 7A), seasonal dynamics are suggested to be limited to offshore wells as indicated by the error bars. The lowest lagoon water fraction is found in the February samples, where, except for J11 ($f_{\text{lag}} = 100\%$), the wells show less than 20% seawater content (Table 1). The February observations are responsible for the increased variation in the offshore wells (Fig. 7A). October, April and July show similar trends amongst all wells, where the shallow onshore wells have less than 10% lagoon water content (Table 1). Among these, July always shows the greatest lagoon water contributions, while the lowest fractions are observed in April (J6–J9) indicating high freshwater influence during that period. October and July fractions show similar trends in the offshore wells with July always containing the greatest lagoon water content.

Mixing fractions observed from the profile of well J5 at the shoreline show a large fraction of lagoon water (50%) at a depth of 10 m below the surface (October). This reached 100% over the next 2 m before gradually decreasing to 0% at 15 m depth (Fig. 7B). Further onshore, at well J4, the same distinct increase in the fraction of lagoon water at the same depth is not repeated, however, at 12 m depth the lagoon water content did increase to be 10% (Fig. 7B). The well compositions are influenced from lagoon water derived from summer intrusions, where EC and $\delta^{18}\text{O}$ enrichment are highest. Furthermore, these results suggest that intruding lagoon water is preserved at greater depths at least until autumn.

4.4. Conceptualization of saltwater intrusion in the near-shore aquifer at Ringkøbing Fjord

Using October as a starting point, a refreshing of the study area is initiated (Fig. 8). Mixing fractions at the offshore wells show high lagoon water content originating from the previous summer, where lagoon water with higher salinities intruded the aquifer. The salinity of the lagoon is around 8 g/L while the average lagoon water level and the groundwater heads between J7–J11 are at 0.1 m.a.s.l and slightly below, respectively, suggesting lagoon water intrusion. Even the limited wave activity present in this system may elevate hydraulic heads of the lagoon increasing the likelihood of saltwater intrusion. On the other hand, the average seepage meter discharge fluxes across the lagoon bed are highest (3.7 cm/d); henceforth terrestrial freshwater input to the lagoon is present.

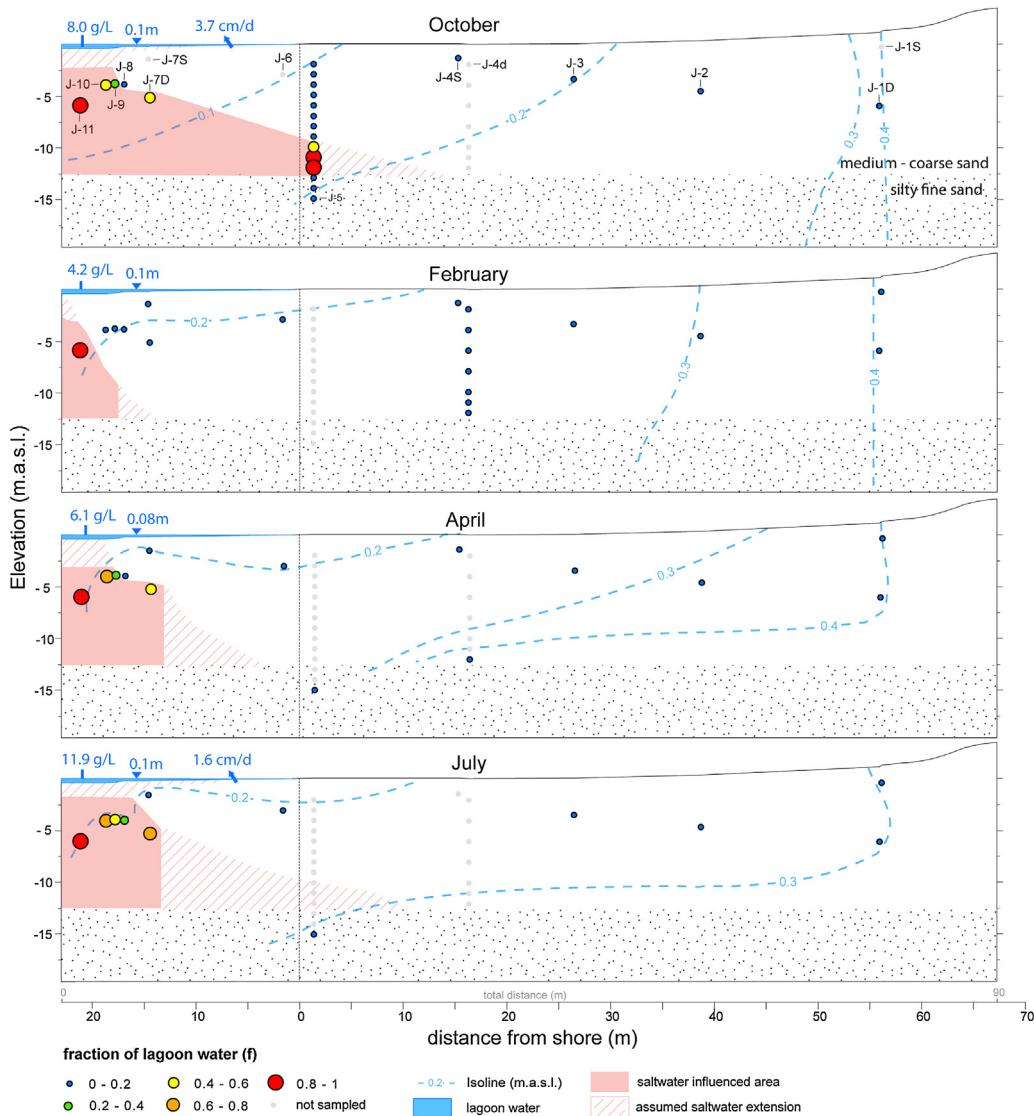


Fig. 8. Conceptualization of the near shore aquifer with corresponding hydraulic head distribution and estimated mixing fractions of lagoon water for different seasons.

The increasing freshwater contribution continues to February as hydraulic heads are on average 10 cm higher (average 0.24 m.a.s.l.) than in October and above lagoon stage (max. 0.1 m.a.s.l.). Thereby, a progression of freshwater input and very low lagoon water salinities (4.2 g/L) produces the lowest observed lagoon water fractions in the wells. Only the most offshore well J11 retains high salinities (Fig. 5). In April the groundwater flux is similar to February (average heads of 0.22 m.a.s.l.). But, due to a salinity increase (6.1 g/L), saltwater begins to slowly intrude again. Towards the summer months, hydraulic heads are slightly reduced and terrestrial SGD inflow is lowered (avg. seepage flux: 1.6 cm/d) by a factor of two, when compared to October (3.7 cm/d). At the same time, increasing salinity due to evaporation and minimal freshwater inputs from groundwater enhances a progressive intrusion of lagoon water.

Moreover, field observations suggest the presence of a low hydraulic conductivity unit around 12 m depth. Such a unit was also reported from earlier studies (Haider, 2013; Kinnear et al., 2013). This unit locally confines the base of upper aquifer and is also believed to be responsible for the high freshwater content seen from mixing fractions in J5 below 14 m depth. Saltwater is limited from intruding this confining unit and consequently is mainly transported inland above the unit. As no saltwater was observed in February at a depth of 12 m a dynamic interface is to be expected at J4.

A seasonal variation of saltwater intrusion pattern was postulated from Robinson et al. (1998), who collected a yearly dataset of head measurements and salinities with one time samples from seepage meters in the Chesapeake Bay, Virginia. They concluded that seasons with low freshwater discharge and high surface water salinities were associated with landward intrusion of saltwater and, vice versa, increased freshwater contribution can be attributed to higher groundwater discharge and low surface water salinities.

However, their study lacks a seasonal observed component of SGD. Seasonal dynamics were also found by Poulsen et al. (2010) at a Danish coastal field site using vertical ERT-profiling, where the annual salinity pattern within the aquifer is modified seasonally as a consequence of an increasing and decreasing freshwater lens due to recharge variations. Yet, at their study site, a change in surface water salinities was not considered. A tracer study conducted in a Mediterranean lagoon system in Turkey showed that, on a larger scale, lagoon water was composed of mainly freshwater derived from lake water upstream of the lagoon during the wet seasons as a consequence of increased hydraulic heads (Stumpp et al., 2014). Whereas during dry seasons, the lagoon water was fed mostly by ocean water due to density-induced inflow, as well as reduced hydraulic heads in the catchment which decreased the freshwater contribution.

Our study, however, is the first to use EC and $\delta^{18}\text{O}$ in a dual-tracer approach with uncertain end-members to quantify seasonal dynamics of SGD and movement of the saltwater–freshwater interface. Jørgensen et al. (2008) used $^{87}\text{Sr}/^{86}\text{Sr}$ and $\delta^{18}\text{O}$ to study saltwater intrusion during a pumping experiment, but did not account for end-member uncertainty. The tracer data corroborates the interpretation of hydraulic gradients and seepage meters results, but additionally provides information regarding internal flow dynamics observed off-shore below the lagoon bed.

Elaborations on the seasonality of saltwater freshwater wedge dynamics are speculative as the data from the lower areas of the aquifer are not sufficient enough to make conclusions. However, based on the observations in the shallow parts of the aquifer, it can be speculated that the replacement of saltwater by freshwater takes place throughout the aquifer down to the low confining unit starting in October. Saltwater intrusion also affects the whole offshore part of the upper aquifer during summer months. Based on observations in the profile wells, the maximum extension of the saltwater wedge toe appears to be located between J5 and J4.

5. Conclusions

A dual-tracer approach using electrical conductivity and water stable isotopes was used to assess and quantify seasonal flow dynamics and the movement of a saltwater–freshwater interface near Ringkøbing Fjord, a coastal lagoon system in Denmark.

The site provides natural conditions to isolate the effects of density-driven subsurface flow and freshwater fluxes on the seasonal development of a saltwater wedge. The lagoon stage is very stable and wedge dynamics are mainly introduced by the seasonal variation of salinities in the lagoon and seasonal varying inland hydraulic gradients. Our study demonstrated that this leads to seawater intrusion during summer conditions (dry period), when salinity is high and hydraulic gradients are low, and a retreating saltwater wedge in the aquifer during winter conditions (wet period), when surface water salinities are low and hydraulic gradients high. The total submarine groundwater discharge to the lagoon varies roughly by a factor of 2–3 between seasons. Flow dynamics and changes in salinity are almost entirely below the lagoon, however, our observations do not provide certain conclusions regarding the seasonal dynamics of the toe location of the saltwater wedge.

In our study a dual tracer end-member analysis was effective in quantifying the saltwater intrusion. The dual-tracer end-member mixing analysis was compared with a single-tracer end-member analysis using only EC (as a cheap measurement of salinity) and $\delta^{18}\text{O}$. We demonstrate that the dual-tracer approach yields different mixing fractions, especially below the lagoon bed, where the system is most dynamic. $\delta^{18}\text{O}$ is a more robust tracer than EC and its end-member concentrations, particularly of lagoon water, are more seasonal stable and improve the estimations of mixing fractions. We show that with the use of EC in a single tracer end-member estimate, lagoon fractions in wells differ 18% on average, with individual wells differing as much as 97%. These variations have the potential to introduce biased conclusions about the lagoon system. By only using $\delta^{18}\text{O}$, differences could be minimized to 6%, but single wells still had differences up to 30% compared to the dual-tracer approach. The performance of a single tracer mixing estimate strongly depends on the right choice of end-member concentration. We believe the MIX-model estimates to be most reliable as the model treats observations as true values, incorporates both tracers simultaneously, and accounts for variances or uncertainties in the end-members.

Consequently, we recommend that when dealing with coastal environments or lagoon settings, where EC of the lagoon is prone to high temporal variations (daily, weekly, monthly), to concurrently apply $\delta^{18}\text{O}$ as a more robust tracer. The simultaneous application of both tracers can improve mixing estimations substantially.

Acknowledgements

This work was supported by the Center for Hydrology (HOBE, www.hobe.dk), funded by the Villum foundation. The research leading to these results has received funding from the European Union Seventh Framework Programme FP7/2007–2013 under Grant Agreement No. 624496. We thank all people helping in the Field and Laboratory, Joakim Stau, Rena Meyer, Jolanta Kazmierczak and H. Badger.

References

- Apello, C.A.J., Postma, D., 2005. *Geochemistry, Groundwater and Pollution*, 2nd ed. Amsterdam <http://dx.doi.org/10.1201/NOE0849338304.ch282>.
- Ataie-Ashtiani, B., Volker, R.E.E., Lockington, D.A.A., 1999. Tidal effects on sea water intrusion in unconfined aquifers. *J. Hydrol.* 216, 17–31. [http://dx.doi.org/10.1016/S0022-1694\(98\)00275-3](http://dx.doi.org/10.1016/S0022-1694(98)00275-3).
- Barlow, P.M., 2003. *Ground water in freshwater–saltwater environments of the Atlantic Coast*. Circular 1262. USGS, Reston, Virginia.
- Barlow, P.M., Reichard, E.G., 2010. Saltwater intrusion in coastal regions of North America. *Hydrogeol. J.* 18, 247–260. <http://dx.doi.org/10.1007/s10040-009-0514-3>.
- Benway, H.M., Mix, A.C., 2004. Oxygen isotopes, upper ocean salinity, and precipitation sources in the eastern tropical Pacific. *Earth Planet. Sci. Lett.* 224, 493–507.

- Burnett, W.C., Taniguchi, M., Oberdorfer, J., 2001. Measurement and significance of the direct discharge of groundwater into the coastal zone. *J. Sea Res.* 46 (2), 109–116. [http://dx.doi.org/10.1016/S1385-1101\(01\)00075-2](http://dx.doi.org/10.1016/S1385-1101(01)00075-2).
- Burnett, W.C., Dulaiova, H., 2003. Estimating the dynamics of groundwater input into the coastal zone via continuous radon-222 measurements. *J. Environ. Radioact.* 69, 21–35. [http://dx.doi.org/10.1016/S0265-931X\(03\)00084-5](http://dx.doi.org/10.1016/S0265-931X(03)00084-5).
- Burnett, W.C., Aggarwal, P.K., Aureli, A., Bokuniewicz, H., Cable, J.E., Charette, M.A., Kontar, E., Krupa, S., Kulkarni, K.M., Loveless, A., Moore, W.S., Oberdorfer, J.A., Oliveira, J., Ozyurt, N., Povinec, P., Privitera, A.M., Rajar, R., Ramesur, R.T., Scholten, J., Stieglitz, T., Taniguchi, M., Turner, J.V., 2006. Quantifying submarine groundwater discharge in the coastal zone via multiple methods. *Sci. Total Environ.* 367 (2–3), 498–543. <http://dx.doi.org/10.1016/j.scitotenv.2006.05.009>.
- Carrera, J., Vazquez-Su, E., Castillo, O., Sanchez-Vila, X., 2004. A methodology to compute mixing ratios with uncertain end-members. *Water Resour. Res.* 40, 1–11. <http://dx.doi.org/10.1029/2003WR002263>.
- Cartwright, N., Li, L., Nielsen, P., 2004. Response of the salt–freshwater interface in a coastal aquifer to a wave-induced groundwater pulse: field observations and modelling. *Adv. Water Resour.* 27, 297–303. <http://dx.doi.org/10.1016/j.advwatres.2003.12.005>.
- Chang, S.W., Clement, T.P., 2012. Experimental and numerical investigation of saltwater intrusion dynamics in flux-controlled groundwater systems. *Water Resour. Res.* 48, 1–10. <http://dx.doi.org/10.1029/2012WR012134>.
- Clark, I.D., Fritz, P., 1997. *Environmental Isotopes in Hydrogeology*. CRC Press/Lewis Publishers.
- DMI (Danish Meteorological Institute), 2017. Haveprognoser. http://www.dmi.dk/hav/udsigter/havprognoser/#tyske_bugt (assessed 07.11.17).
- Duque, C., Müller, S., Sebok, E., Haider, K., Engesgaard, P., 2016. Estimating groundwater discharge to surface waters using heat as a tracer in low flux environments: the role of thermal conductivity. *Hydrol. Process.* 30, 383–395. <http://dx.doi.org/10.1002/hyp.10568>.
- EEA, 2012. <http://www.eea.europa.eu/data-and-maps/figures/mean-tidal-amplitude>.
- Gat, J.R., 2010. *Isotope Hydrology: A Study of the Water Cycle, Series on*. Imperial College Press, London.
- Gonfiantini, R., 1986. Environmental isotopes in lake studies. In: Fritz, P., Fontes, J.C. (Eds.), *Handbook of Environmental Isotope Geochemistry*, vol. 2: The Terrestrial Environment, B. Elsevier, pp. 113–168. <http://dx.doi.org/10.1016/B978-0-444-42225-5.50008-5>.
- Craig, H., 1961. Isotopic variation in meteoric waters. *Science* 133, 1702–1703.
- Haider, K., 2013. Numerical and Experimental Investigations of Submarine Groundwater Discharge to a Coastal Lagoon (Ph.D. thesis). University of Copenhagen, Copenhagen.
- Haider, K., Engesgaard, P., Sonnenborg, T.O., Kirkegaard, C., 2014. Numerical modeling of salinity distribution and submarine groundwater discharge to a coastal lagoon in Denmark based on airborne electromagnetic data. *Hydrogeol. J.* 23, 217–233. <http://dx.doi.org/10.1007/s10040-014-1195-0>.
- Haines, P., 2006. Physical and chemical behaviour and management of Intermittently Closed and Open Lakes and Lagoons (ICOLLs) in NSW Griffith Centre for Coastal Management School of Environmental and Applied Sciences Doctor of Philosophy. Environmental and Applied Sciences Griffith University.
- Haralambidou, K., Sylaios, G., Tsihrintzis, V.A., 2010. Salt-wedge propagation in a Mediterranean micro-tidal river mouth. *Estuar. Coast. Shelf Sci.* 90, 174–184. <http://dx.doi.org/10.1016/j.ecss.2010.08.010>.
- Holzbecher, E.O., 1998. *Modeling Density-Driven Flow in Porous Media: Principles, Numerics, Software, Bind 1*.
- Jørgensen, N.O., Andersen, M.S., Engesgaard, P., 2008. Investigation of a dynamic seawater intrusion event using strontium isotopes ($^{87}\text{Sr}/^{86}\text{Sr}$). *J. Hydrol.* 348 (3–4), 257–269. <http://dx.doi.org/10.1016/j.jhydrol.2007.10.001>.
- Kendall, C., Caldwell, E.A., 1998. Fundamentals of isotope geochemistry. *Isotope Tracers in Catchment Hydrology*. pp. 5186. <http://dx.doi.org/10.1016/B978-0-444-81546-0.50009-4>. (chapter 2).
- Kinnear, J.A., Binley, A., Duque, C., Engesgaard, P.K., 2013. Using geophysics to map areas of potential groundwater discharge into Ringkøbing Fjord, Denmark. *Lead. Edge* 32, 792–796. <http://dx.doi.org/10.1190/le32070792.1>.
- Kirkegaard, C., Sonnenborg, T.O., Auker, E., Jørgensen, F., 2011. Salinity distribution in heterogeneous coastal aquifers mapped by airborne electromagnetics. *Vadose Zone J.* 10, 125. <http://dx.doi.org/10.2136/vzj2010.0038>.
- Kjerfve, B., 1994. Coastal lagoon processes. *Elsevier Oceanogr. Ser.* 60, 18. <http://dx.doi.org/10.1201/EBK1420088304-c1>.
- Kurup, G.R., Hamilton, D.P., Patterson, J.C., 1998. Modelling the effect of seasonal flow variations on the position of salt wedge in a microtidal estuary. *Estuar. Coast. Shelf Sci.* 47, 191–208. <http://dx.doi.org/10.1006/ecss.1998.0346>.
- Lee, D.R., 1977. A device for measuring seepage flux in lakes and estuaries. *Limnol. Oceanogr.* 22, 140–147. <http://dx.doi.org/10.4319/lo.1977.22.1.0140>.
- Leibundgut, C., Maloszewski, P., Külls, C., 2009. Tracers in hydrology. *Tracers Hydrol.* <http://dx.doi.org/10.1002/9780470747148>.
- Li, L., Barry, D.A., Stagnitti, F., Parlange, J.Y., 1999. Submarine groundwater discharge and associated chemical input to a coastal sea. *Water Resour. Res.* 35, 3253–3259. <http://dx.doi.org/10.1029/1999WR900189>.
- McConnell, M.C., Thunell, R.C., Lorenzoni, L., Astor, Y., Wright, J.D., Fairbanks, R., 2009. Seasonal variability in the salinity and oxygen isotopic composition of seawater from the Cariaco Basin, Venezuela: Implications for paleosalinity reconstructions. *Geochem. Geophys. Geosyst.* 10.
- Michael, H., Lubetsky, J.S., Harvey, C., 2003. Characterizing submarine groundwater discharge: a seepage meter study in Waquoit Bay, Massachusetts. *Geophys. Res. Lett.* 30 (6). <http://dx.doi.org/10.1029/2002GL016000>.
- Michael, H., Mulligan, A.E., Harvey, C.F., 2005. Seasonal oscillations in water exchange between aquifers and the coastal ocean. *Nature* 436, 1145–1148. <http://dx.doi.org/10.1038/nature03935>.
- Müller, S., Stumpp, C., Sørensen, J.H., Jessen, S., 2017. Spatiotemporal variation of stable isotopic composition in precipitation: post-condensational effects in a humid area. *Hydrol. Process.* 31 (18), 3146–3159.
- Post, V., Kooi, H., Simmons, C., 2007. Using hydraulic head measurements in variable-density ground water flow analyses. *Ground Water* 45 (6), 664–671. <http://dx.doi.org/10.1111/j.1745-6584.2007.00339.x>.
- Poulsen, S.E., Rasmussen, K.R., Christensen, N.B., Christensen, S., 2010. Evaluating the salinity distribution of a shallow coastal aquifer by vertical multielectrode profiling (Denmark). *Hydrogeol. J.* 18, 161–171. <http://dx.doi.org/10.1007/s10040-009-0503-6>.
- Phleger, F.B., Zimmermann, J.P.F., Allen, G., Nichols, M., Mandelli, E., Krumbein, W.E., Lasserre, P., 1981. Coastal lagoon research, present and future. *Proceedings of a Seminar. UNESCO Technical Papers in Marine Science* 32 94.
- Price, M., Stewart, P.K., Price, R.M., 2003. Use of tritium and helium to define groundwater flow conditions in Everglades National Park. *Water Resour. Res.* 39, 1–12. <http://dx.doi.org/10.1029/2002WR001929>.
- Robinson, M., Gallagher, D., Reay, W., Gallagher, D., Reay, W., 1998. Field observations of tidal and seasonal variations in groundwater discharge to tidal estuarine surface water. *Gr. Water Monit. Remediat.* 18, 83–92. <http://dx.doi.org/10.1111/j.1745-6592.1998.tb00605.x>.
- Singh, A., Jani, R.A., Ramesh, R., 2010. Spatiotemporal variations of the $\delta^{18}\text{O}$ -salinity relation in the northern Indian Ocean. *Deep-Sea Res. Part I: Oceanogr. Res. Pap.* 57 (11), 1422–1431. <http://dx.doi.org/10.1016/j.dsr.2010.08.002>.
- Spruill, T.B., Bratton, J.F., 2008. Estimation of groundwater and nutrient fluxes to the Neuse River estuary, North Carolina. *Estuar. Coasts* 31 (3), 501–520. <http://dx.doi.org/10.1007/s12237-008-9040-0>.
- Stumpp, C., Ekdal, A., Gönenc, I.E., Maloszewski, P., 2014. Hydrological dynamics of water sources in a Mediterranean lagoon. *Hydrol. Earth Syst. Sci.* 18, 4825–4837. <http://dx.doi.org/10.5194/hess-18-4825-2014>.
- Taniguchi, M., Burnett, W.C., Cable, J.E., Turner, J.V., 2002. Investigation of submarine groundwater discharge. *Hydrol. Process.* 16, 2115–2129. <http://dx.doi.org/10.1002/hyp.1145>.
- Woodroffe, C.D., 2002. *Coasts: Form, Process and Evolution*. Cambridge University Press.
- Werner, A.D., Bakker, M., Post, V.E.A.A., Vandenbohede, A., Lu, C., Ataie-Ashtiani, B., Simmons, C.T., Barry, D.A., 2013. Seawater intrusion processes, investigation and management: recent advances and future challenges. *Adv. Water Resour.* 51, 3–26. <http://dx.doi.org/10.1016/j.advwatres.2012.03.004>.
- Yurtsever, Y., 1997. *Role of Environmental Isotopes in Studies Related to Salinization Process and Saltwater Intrusion Dynamics*. IAEA, Vienna.